

Low-loss high-index-contrast planar waveguides with graded-index cladding layers

Juejun Hu¹, Ning-Ning Feng^{1*}, Nathan Carlie², Laeticia Petit², Jianfei Wang¹,
Anu Agarwal^{1*}, Kathleen Richardson², and Lionel Kimerling¹

¹Microphotonics Center, Massachusetts Institute of Technology, Cambridge, Massachusetts 02139, USA

²Advanced Materials Research Laboratory, Clemson University, Anderson, South Carolina 29625, USA

*Corresponding authors: anu@mit.edu, fengn@mit.edu

Abstract: We experimentally demonstrate, for the first time, propagation loss reduction via graded-index (GRIN) cladding layers in high-index-contrast (HIC) glass waveguides. We show that scattering loss arising from sidewall roughness can be significantly reduced without compromising the high-index-contrast condition, by inserting thin GRIN cladding layers with refractive indices intermediate between the core and topmost cover of a strip waveguide. Loss as low as 1.5 dB/cm is achieved in small core ($1.6 \mu\text{m} \times 0.35 \mu\text{m}$), high-index-contrast ($\Delta n = 1.37$) arsenic-based sulfide strip waveguides. This GRIN cladding design is generally applicable to HIC waveguide systems such as Si/SiO₂.

©2007 Optical Society of America

OCIS codes: (130.2790) Guided waves; (130.3120) Integrated optics devices; (160.2750) Glass and other amorphous materials; (230.7380) Waveguides, channeled; (240.5770) Roughness; (310.1860) Deposition and fabrication.

References and links

1. C. A. Barrios and M. Lipson, "Electrically driven silicon resonant light emitting device based on slot-waveguide," *Opt. Express* **13**, 10092 (2005).
2. Q. Xu, V. R. Almeida, and M. Lipson, "Demonstration of high Raman gain in a submicrometer-size silicon-on-insulator waveguide," *Opt. Lett.* **30**, 35-37 (2005).
3. T. Barwicz and H. Haus, "Three-dimensional analysis of scattering losses due to sidewall roughness in microphotonic waveguides," *J. Lightwave Technol.* **23**, 2719-2732 (2005).
4. M. Webster, R. Pafchek, G. Sukumaran, and T. Koch, "Low-loss quasi-planar ridge waveguides formed on thin silicon-on-insulator," *Appl. Phys. Lett.* **87**, 231108-231110 (2005).
5. D. Sparacin, S. Spector, and L. Kimerling, "Silicon Waveguide Sidewall Smoothing by Wet Chemical Oxidation," *J. Lightwave Technol.* **23**, 2455-2461 (2005).
6. K. Lee, D. Lim, L. Kimerling, J. Shin, and F. Cerrina, "Fabrication of ultralow-loss Si/SiO₂ waveguides by roughness reduction," *Opt. Lett.* **26**, 1888-1890 (2001).
7. M. Wu and M. Lee, "Thermal annealing in hydrogen for 3-D profile transformation on silicon-on-insulator and sidewall roughness reduction," *J. Microelectromech. Syst.* **15**, 338-343 (2006).
8. C. Chao and L. Guo, "Reduction of surface scattering loss in polymer microrings using thermal-reflow technique," *IEEE Photon. Technol. Lett.* **16**, 1498-1500 (2004).
9. J. Hu, V. Tarasov, N. Carlie, R. Sun, L. Petit, A. Agarwal, K. Richardson, and L. Kimerling, "Low-loss integrated planar chalcogenide waveguides for chemical sensing," *Proc. SPIE* **6444**, 64440N (2007).
10. J. Hu, V. Tarasov, N. Carlie, N. Feng, L. Petit, A. Agarwal, K. Richardson, and L. Kimerling, "Si-CMOS-compatible lift-off fabrication of low-loss planar chalcogenide waveguides," *Opt. Express* **15**, 11798 (2007).
11. M. Richardson, L. Shah, J. Tawney, A. Zoubir, C. Rivera, C. Lopez, and K. Richardson, "Photo-induced structural changes in glass," *Glass Sci. Technol.* **75**, 121-130 (2002).
12. P. Lucas, D. Le Coq, C. Juncker, J. Collier, D. Boesewetter, C. Boussard-Pledel, B. Bureau, M. Riley, "Evaluation of toxic agent effects on lung cells by fiber evanescent wave spectroscopy," *Appl. Spectrosc.* **59**, 1-9 (2005).
13. M. Asobe, H. Itoh, T. Miyazawa, and T. Kanamori, "Efficient and ultrafast all-optical switching using high Δn , small core chalcogenide glass fibre," *Electron. Lett.* **29**, 1966-1968 (1993).
14. J. Hu, L. Petit, X. Sun, A. Agarwal, N. Carlie, T. Anderson, J. Choi, J. Viens, M. Richardson, K. Richardson, and L. Kimerling, "Studies on Structural, Electrical and Optical Properties of Cu-doped As-Se-Te Chalcogenide Glasses," *J. Appl. Phys.* **101**, 063520-063528 (2007).
15. D. Sparacin, R. Sun, A. Agarwal, M. Beals, J. Michel, L. Kimerling, T. Conway, A. Pomerene, D. Carothers, M. Grove, D. Gill, M. Rasras, S. Patel, A. White, "Low-Loss Amorphous Silicon Channel

Waveguides for Integrated Photonics,” in *Proceedings of 3rd IEEE International Conference on Group IV Photonics*, pp. 255-257.

16. N. Feng, G. Zhou, C. Xu, and W. Huang, “Computation of full-vector modes for bending waveguide using cylindrical perfectly matched layers,” *IEEE J. Lightwave Technol.* **20**, 1976-1980 (2002).
17. L. Petit, N. Carlie, F. Adamietz, M. Couzi, V. Rodriguez, and K. C. Richardson, “Correlation between physical, optical and structural properties of sulfide glasses in the system Ge-Sb-S,” *Mater. Chem. Phys.* **97**, 64-70 (2006).
18. J. Hu, V. Tarasov, N. Carlie, L. Petit, A. Agarwal, K. Richardson, and L. Kimerling, “Fabrication and Testing of Planar Chalcogenide Waveguide Integrated Microfluidic Sensor,” *Opt. Express* **15**, 2307 (2007).

1. Introduction

High-index-contrast (HIC) strip waveguides (typically with a core-cladding index difference $\Delta n > 1$) comprise a key component in integrated microphotonics. Compared to their low-index-contrast (LIC) counterparts, these waveguides allow tight bending structures and small device footprint with minimized inter-guide cross talk, both essential features to compact planar photonic integration. Furthermore, the tight confinement and hence small modal volume in HIC waveguides is also critical to the operation of a number of photonic devices, including on-chip light sources [1] and nonlinear optical devices [2]. Despite these apparent advantages, the high loss in HIC waveguides arising from sidewall roughness scattering has been a major limiting factor in HIC waveguide device development. Sidewall roughness scattering is particularly severe for HIC waveguides, since the scattering loss scales with index difference [3]. LIC waveguides or rib waveguides suffer much less sidewall roughness scattering and typically exhibit lower propagation loss [4] but they lack the aforementioned HIC-device advantages. Thus to make HIC devices viable, an effective solution is to develop surface smoothing techniques to remove sidewall roughness. A number of methods have been demonstrated in different material systems for waveguide surface roughness reduction, including oxidation smoothing [5], post-fabrication wet etching [6] and hydrogen annealing [7] in Si/SiO₂ systems, and reflow in polymer [8] and glass materials [9]. However, some of these methods involve high temperature processing and hence pose integration challenges with other planar photonic and electronic devices. To maintain the advantage of planar integration over a wide range of material systems, an efficient loss reduction technique that is universally applicable to all HIC material systems is highly desirable.

Here we present a novel loss reduction scheme involving a graded index (GRIN) cladding design. Although we successfully demonstrate the design concept in As₄₂S₅₈ chalcogenide strip waveguides, this design can be applied to any other HIC material system as well, provided that suitable graded index cladding layer compositions can be identified. Traditionally GRIN configuration and index profile engineering have been widely employed in fiber formation to minimize modal dispersion. In a planar configuration, GRIN structures are naturally formed in a number of diffusion-based processes typified by ion exchange. However, waveguides formed by ion-exchange typically exhibit an index contrast smaller than 0.1, and thus roughness scattering is often not a major concern to be addressed. Instead of using diffusion-based technology, in this paper, the high-index-contrast As₄₂S₅₈ strip waveguides are fabricated on a silicon platform via lift-off, a process compatible with high-volume complimentary-metal-oxide-semiconductor (CMOS) fabrication, as we have recently demonstrated [10]. The reason to use glassy materials in this demonstration is three-fold: the amorphous nature of chalcogenide glasses (ChG's) facilitates the deposition of multi-layer thin films on the same substrate without lattice match constraints; glass alloys with different compositions provide a wide range of refractive index values (Table 1), offering the possibility of continuous index variation for different core to cladding material combinations; and ChG's have received considerable attention for applications in microphotonic devices in recent years due to their unique properties such as high infrared transparency, large optical nonlinearity, capability of variations of properties, almost unlimited ability for alloying, and photosensitivity [11]. Fiber-based photonic devices such as fiber optical sensors [12] and all-optical switches [13], which utilize these unique properties of ChG's, have already been demonstrated. Nevertheless, planar chalcogenide waveguide-based devices remain much less

explored, despite their distinct advantages over their fiber counterparts, including superior mechanical robustness, ease of integration with other on-chip devices and the ability to take advantage of economies of scale enabled by leveraging on large-scale wafer processing. A major hurdle towards realization of these planar devices still remains the relatively high optical loss in waveguides compared to fibers, and thus loss reduction designs are highly desirable. In this paper, we demonstrate effective transmission loss reduction in $\text{As}_{42}\text{S}_{58}$ waveguides through the application of GRIN cladding layers.

Table 1. Range of refractive indices of some glassy alloys for potential GRIN cladding applications.

Alloy system	Refractive index range
PECVD SiON (silicon oxynitride)	1.44 – 2.26*
Thermally evaporated As_2S_3 - As_2Se_3	2.39 – 2.82*
Thermally evaporated Ge-Sb-S-Se	2.06 – 2.76*
Co-evaporated As_2Se_3 -CuSe	2.82 – 2.97 ¹⁴

*From our own measurement results.

2. Graded-index cladding waveguide modal analysis

According to volume current theory [3], the scattering loss from waveguide sidewalls is proportional to the equivalent polarization current densities on rough surfaces:

$$\vec{J}_{rough}(\vec{r}) = -j\omega\epsilon_0\delta n^2(\vec{r})\vec{E}_g(\vec{r}) \quad (1)$$

where δn [2] is the refractive index deviation from perfectly smooth waveguide due to sidewall roughness, and E_g is the guided mode of the smooth waveguide. The index deviation δn^2 is directly related to roughness amplitude as well as index difference between core and cladding. The equation indicates two ways to reduce the scattering loss caused by the equivalent surface current, J_{rough} : reducing the index deviation (i.e. reducing roughness or index contrast) or reducing the field E_g at interfaces. Reducing surface field amplitude E_g through careful waveguide design can minimize the interaction of optical mode and rough waveguide sidewall. Adiabatically increasing waveguide width is one solution reported previously [15]. However, multi-mode effects limit the application of this scheme to straight waveguides without bends.

Here we present a more universal approach using a graded index cladding design. Both index contrast δn [2] and surface field amplitude E_g can be reduced simultaneously simply by sandwiching thin layers of intermediate refractive indices between the high-index waveguide core and the low-index topmost cover. Figure 1(a) shows the cross-sectional schematic of an $\text{As}_{42}\text{S}_{58}$ ($n = 2.37$) strip waveguide coated with $\text{Ge}_{17}\text{Sb}_{12}\text{S}_{71}$ ($n = 2.06$) / SiO_2 ($n = 1.46$) double GRIN cladding layers. The $\text{As}_{42}\text{S}_{58}$ waveguide core sitting on SiO_2 under cladding has a width of $0.75 \mu\text{m}$ and a height of $0.35 \mu\text{m}$. Both $\text{Ge}_{17}\text{Sb}_{12}\text{S}_{71}$ and oxide GRIN cladding layers have a thickness of 35 nm each. A cross-sectional view of the field along x-axis at the waveguide center of the quasi-TE mode is shown in Fig. 1(b), together with the field distribution in the absence of GRIN cladding layers for comparison, both computed using a full-vectorial mode solver with perfectly matched layer (PML) boundary [16]. It is evident that GRIN cladding layers decrease the field amplitude at the core/cladding interface. In an ideal case the post-etch deposited oxide layer should have negligible surface roughness, and a theoretical analysis using volume current theory taking into account the different radiation efficiency of current sources on GRIN layer interfaces has predicted a quasi-TE mode loss reduction of 55% for the $\text{As}_{42}\text{S}_{58}$ waveguide structure shown in Fig. 1(a), compared to waveguides without GRIN cladding layers. It should be noted though, that if the GRIN cladding layers have rough surfaces, the desired effect of loss reduction may be partially cancelled out.

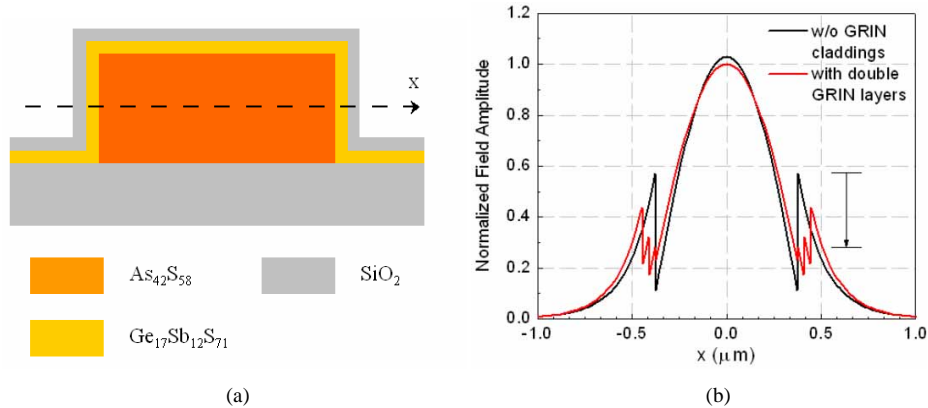


Fig. 1. (a). Cross-sectional schematic of an $\text{As}_{42}\text{S}_{58}$ waveguide with $\text{Ge}_{17}\text{Sb}_{12}\text{S}_{71}/\text{SiO}_2$ double GRIN cladding layers; (b) cross-sectional view of the field along x-axis of the quasi-TE mode in the same structure with (red) and without (black) GRIN cladding layers, showing field intensity decrease at the interfaces.

One important feature of the GRIN cladding design is the reduction of index contrast, and hence scattering loss, while still maintaining highly confined optical guiding, featured by strong optical power confinement in the waveguide core and the ability to tolerate tight bends. Figure 2(a) compares simulated bending losses of quasi-TE modes as a function of bending radius in waveguides with and without GRIN cladding layers. It is clear that waveguide bending loss decreases with the incremental addition of GRIN cladding layers, an essential requirement from compact planar photonic integration.

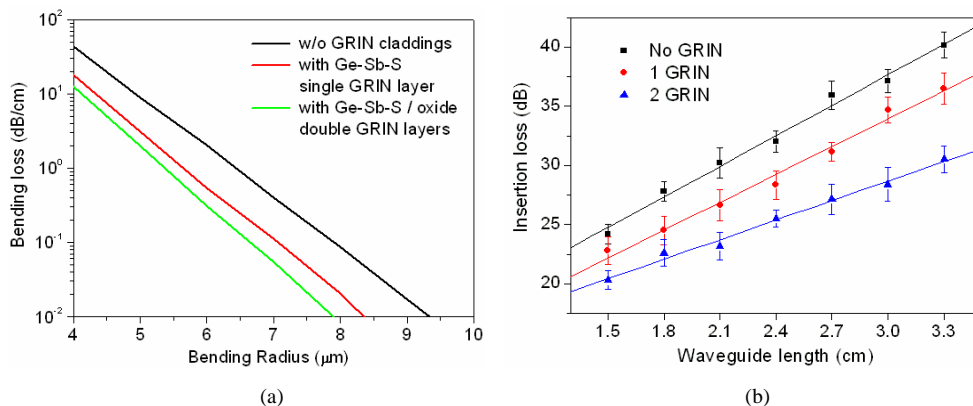


Fig. 2. (a). Bending loss of quasi-TE mode as a function of bending radius in waveguides with and without GRIN cladding at 1550 nm wavelength, indicating that GRIN design also improves waveguide bending performance besides loss reduction; (b) measured insertion loss data of the $0.75\ \mu\text{m}$ $\text{As}_{42}\text{S}_{58}$ waveguides with and without GRIN cladding layers, the slopes of the fitted lines represent measured waveguide loss.

3. Waveguide fabrication and characterization

3.1 Waveguide fabrication

Bulk chalcogenide glasses are prepared using a traditional chalcogenide melt-quenching technique. From this bulk high-quality thin films are deposited onto $3\ \mu\text{m}$ -thick oxide-coated Si wafers (Silicon Quest International Inc.) using thermal evaporation. Details of the bulk sample preparation and film deposition process may be found elsewhere [17, 18]. The refractive index of the as-evaporated films at 1550 nm wavelength is determined using a Metricon 2010 prism coupler. In this study, the waveguide core is made of thermally

evaporated $\text{As}_{42}\text{S}_{58}$ ($n = 2.37$). Thermally evaporated $\text{Ge}_{17}\text{Sb}_{12}\text{S}_{71}$ film ($n = 2.06$) and sputtered silicon dioxide ($n = 1.46$) are chosen as the GRIN layers. $\text{As}_{42}\text{S}_{58}$ waveguides with a core height of 350 nm and three different width, 0.75 μm , 1.2 μm and 1.6 μm are fabricated using lift-off technique on a 500 nm CMOS line. The lift-off process has been described in detail elsewhere [10]. The GRIN layers are subsequently deposited on patterned waveguides to form conformal coatings over the $\text{As}_{42}\text{S}_{58}$ core. It is worth pointing out that argon gas is intentionally introduced into deposition chamber during $\text{Ge}_{17}\text{Sb}_{12}\text{S}_{71}$ GRIN cladding evaporation in order to maintain the evaporated gas phase in a viscous flow regime and thus leads to uniform step coverage. Both $\text{Ge}_{17}\text{Sb}_{12}\text{S}_{71}$ and oxide GRIN cladding layers have a thickness of 35 nm each.

Figure 3(a) shows a top view SEM image of a bent section of a 0.75 μm wide GRIN cladding waveguide, indicating excellent pattern fidelity from the lift-off process, and a cleaved waveguide facet in Fig. 3(b) shows the GRIN cladding layers over the $\text{As}_{42}\text{S}_{58}$ core.

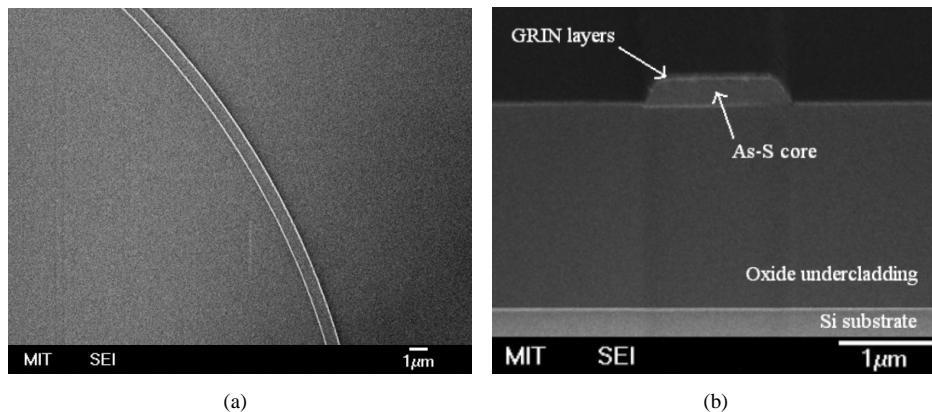


Fig. 3. (a). Top-view SEM image of a 0.75 μm wide $\text{As}_{42}\text{S}_{58}$ waveguide bending section showing excellent pattern fidelity from lift-off; (b) Tilted view of a cleaved facet of a $\text{As}_{42}\text{S}_{58}$ waveguide coated with $\text{Ge}_{17}\text{Sb}_{12}\text{S}_{71}$ and oxide double GRIN layers.

3.2 Waveguide characterization

Waveguide transmission loss measurements are performed on a Newport AutoAlign workstation in combination with a JDSU SWS tunable laser. Lens-tip fibers are used to couple light from the laser into and out of the waveguides. Reproducible coupling between waveguides and fibers is achieved via an automatic alignment system with a spatial resolution better than 50 nm. Optical loss in the waveguides is measured by a cutback method using paper-clip waveguide patterns. Loss measurements on $\text{As}_{42}\text{S}_{58}$ waveguides without GRIN cladding layers are repeated twice consecutively to make sure no oxidation effects interfere with the measurement. Each loss number reported in this paper is averaged over > 25 waveguides. Roughness of the multiple interfaces between core and GRIN cladding layers is measured using a Digital Instruments Nanoscope IIIa Atomic Force Microscope (AFM), yielding RMS roughness values of (10 ± 2) nm, (10 ± 2) nm and (8 ± 2) nm for $\text{As}_{42}\text{S}_{58}$ - $\text{Ge}_{17}\text{Sb}_{12}\text{S}_{71}$ interface, $\text{Ge}_{17}\text{Sb}_{12}\text{S}_{71}$ -oxide interface and oxide surface, respectively. The scans are performed parallel to the direction of the waveguides using the tapping mode.

4. Results and discussion

Measured transmission losses at 1550 nm wavelength, in $\text{As}_{42}\text{S}_{58}$ waveguides without GRIN cladding layers, $\text{As}_{42}\text{S}_{58}$ waveguides coated with a single $\text{Ge}_{17}\text{Sb}_{12}\text{S}_{71}$ GRIN layer, and waveguides coated with $\text{Ge}_{17}\text{Sb}_{12}\text{S}_{71}/\text{SiO}_2$ bilayers, are shown in Table 2. Figure 2(b) shows the insertion loss of quasi-TE mode for the 0.75 μm wide waveguides. The experimental error arising from non-uniformities is estimated to be $\pm 10\%$ of the measured waveguide loss.

Generally it is evident that GRIN cladding structures significantly reduce waveguide loss, and addition of more GRIN cladding layers minimizes loss by further decreasing index and field discontinuities. After the addition of double GRIN cladding layers, quasi-TE mode loss in the 0.75 μm wide waveguides is decreased by 36% compared to the theoretically predicted 55% reduction, and this difference results from the residual roughness on the oxide layer surface. A few observations can be made based on the measurement data: 1) transmission loss increases as waveguide width decreases for both TE and TM polarizations in accordance with our previous study [12]; 2) TE modes are generally more lossy than corresponding TM modes although the difference diminishes as waveguide width increases or when GRIN cladding layers are applied; 3) loss reduction through GRIN cladding design is generally more significant for TE polarization. Both results 1) and 2) can be correlated to the conclusion that sidewall roughness is a major source of optical loss in these HIC waveguides. Similarly, since TE modes suffer more from sidewall scattering than do TM modes, TE modes exhibit larger loss reduction resulting from GRIN cladding layers.

Table 2. Measured optical transmission losses of $\text{As}_{42}\text{S}_{58}$ strip waveguides without GRIN cladding layers (denoted as “No GRIN”), $\text{As}_{42}\text{S}_{58}$ waveguides coated with a single $\text{Ge}_{17}\text{Sb}_{12}\text{S}_{71}$ layer (denoted as “1 GRIN”) and waveguides coated with $\text{Ge}_{17}\text{Sb}_{12}\text{S}_{71}/\text{SiO}_2$ bilayers (denoted as “2 GRIN”) at 1550 nm for three different waveguide widths.

Transmission loss (dB/cm)	0.75 μm		1.2 μm		1.6 μm	
	TM	TE	TM	TE	TM	TE
No GRIN	6.8	8.6	3.9	5.0	2.6	4.4
1 GRIN	6.2	7.9	2.7	3.7	2.2	3.4
2 GRIN	4.8	5.5	2.1	2.6	1.5	1.8

5. Conclusion

We have experimentally demonstrated, for the first time, waveguide loss reduction using a graded-index cladding design. By conformally coating as-fabricated $\text{As}_{42}\text{S}_{58}$ waveguides with thin layers of glasses with lower refractive indices, the index and optical field discontinuity at waveguide core-cladding interfaces is minimized, which leads to significantly reduced transmission losses. Loss value as low as 1.5 dB/cm is obtained in small core (1.6 $\mu\text{m} \times 0.35 \mu\text{m}$), high-index-contrast ($\Delta n = 1.37$) $\text{As}_{42}\text{S}_{58}$ strip waveguides with a double-layer GRIN structure. As our modal analysis has demonstrated, such GRIN designs provide a non-material-specific solution for reducing waveguide loss in high-index-contrast waveguides without compromising the requirements of tight optical confinement and compact optical guiding structures. By combining the GRIN cladding design with other post-fabrication surface smoothing techniques, HIC waveguides with much lower loss figures can be produced. Such low-loss structures can be applied in a number of technical fields such as intra-chip interconnect, biochemical sensing, optical delay lines and planar photonic device processing.

Acknowledgments

Funding support is provided by the Department Of Energy under award number DE-SC52-06NA27341. The authors would like to thank Dr. Jurgen Michel and Dr. Tymon Barwicz at MIT for helpful discussions. The authors also acknowledge the Microsystems Technology Laboratories at MIT for fabrication facilities and the Center for Materials Science and Engineering at MIT for characterization facilities.

Disclaimer

This paper was prepared as an account of work supported by an agency of the United States Government. Neither the United States Government nor any agency thereof, nor any of their employees, makes any warranty, express or implied, or assumes any legal liability or responsibility for the accuracy, completeness or usefulness of any information, apparatus, product or process disclosed, or represents that its use would not infringe privately owned rights. Reference herein to any specific commercial product, process, or service by trade name, trademark, manufacturer, or otherwise does not necessarily constitute or imply its

endorsement, recommendation, or favoring by the United States Government or any agency thereof. The views and opinions of authors expressed herein do not necessarily state or reflect those of the United States Government or any agency thereof.